Institut de Physique Nucléaire de Lyon

Université Claude Bernard

IN2P3 - CNRS

LYCEN 9643
Décembre 1996

Non-Baryonic Dark Matter

Ecole Internationale de Cosmologie, Casablanca, 1-10 décembre 1996

I. Berkès

Institut de Physique Nucléaire de Lyon, IN2P3/CNRS, Université Claude Bernard,
F-69622 Villeurbanne Cedex, France

43, Boulevard du 11 Novembre 1918 - 69622 VILLEURBANNE Cedex - France

NON-BARYONIC DARK MATTER. (*)

I. Berkes
IPNL, Université Lyon I et IN2P3, F-69622 VILLEURBANNE CEDEX

Abstract. This article discusses the nature of the dark matter and the possibility of the detection of non-baryonic dark matter in an underground experiment. Among the useful detectors the low temperature bolometers are considered in some detail.

Résumé. Cet article expose les différentes hypothèses sur la nature de la matière noire, et la possibilité de la détection de la matière noire non-baryonique dans une expérience souterraine. Parmi les détecteurs envisagés l'accent est mis sur les bolomètres travaillant à basse température.

1) Galactic dark matter.

The best known star in our Galaxy is the Sun. Its mass is about $M_\odot = 2 \times 10^{30}$ kg, and it radiates a power of $L_\odot = 3.8 \times 10^{26}$ W. The ratio of these two quantities is $M_\odot/L_\odot = 5200$ kg/W. In our Galaxy masses for binary stars can be determined from their relative movement. It comes out, that while M and L vary strongly from a star to another, the ratio M/L varies only slightly for stars in the main sequence. So, the luminosity may be used as a mesure o the mass of a star, super-giants, white dwarfs, black holes and other exoti objects excepted. The mass to light ratio of astronomical objects is generally expressed in this solar unit as $M/L = 1 (M_\odot/L_\odot)$.

Most of the bright galaxies, so also our Milky Way, are spiral galaxies. The centre of the galaxy is occupied by a bulge. In our Galaxy this bulge is now considered as a triaxial bar, with half axes of 1.5, 0.6 and 0.4 kpc, concentrating about 2×10^{10} solar masses [1]. Two (or more) flat arms are disposed inside a flat disk around the bulge.

According to the importance of the bulge with respect to the disk, galaxies are classified in Sa, Sb, Sc and Sd types. The Milky Way is rather of Sb type. In the Milky Way the total extension of the luminous matter, the optical radius is about 15 kpc. The stars in the disk are younger (population I), than those contained in the bulge (population II).

The thickness of the disk is about 1 kpc. The Sun is at about 8.5 kpc from the galactic centre, and distant only 25 pc from the symmetry plane of the disk. The ecliptic is tilted to 60.2° with respect to the galactic plane. This localization allows to see many stars, in both directions, towards the galactic centre and also in the opposite direction. Unfortunately, on account of the galactic dust, we see optically only a small part of our own Galaxy.

Spiral galaxies rotate. We shall come back later in more detail on this movement. Just in order to fix ideas: the rotation speed of the Sun around the galactic centre is $v_\odot = 220$ km/s.

A low density, nearly spherical halo, composed from some stars and globular clusters surrounds the Milky Way. This halo rotates slowly, its rotation speed near the Sun is about 50 km/s.

Atomic H is easily detected by its characteristic radio emission of 21 cm wavelength. This gaz can be seen even very far from the optical radius, thus increasing the observable dimensions of the Galaxy. Very few of this gaz is in the galactic centre. Neutral (H I)and ionized hydrogen and molecular hydrogen gaz (very difficult to observe) are estimated to represent about 10 % of the total galactic mass.

Doppler shift of the light, emitted by galaxies disposed edge-on with respect to the observation direction, establishes the rotation velocity versus distance from galaxy centre relations, the so called rotation curves. In fig. 1 we show a typical example of such a rotation curve and its analysis, taken from ref. 2. For certain galaxies these curves are somewhat different: as for the Milky Way, after a maximum the velocity drops a little bit, then it stabilizes. Atomic hydrogen rotation can be observed even

---

* Remark.
Some general references, as books, review articles, containing long reference lists, are not referenced to throughout this text. They are given separately in the first part of the reference list.

at twice the optical radius, and it shows the same, nearly constant circular velocity.

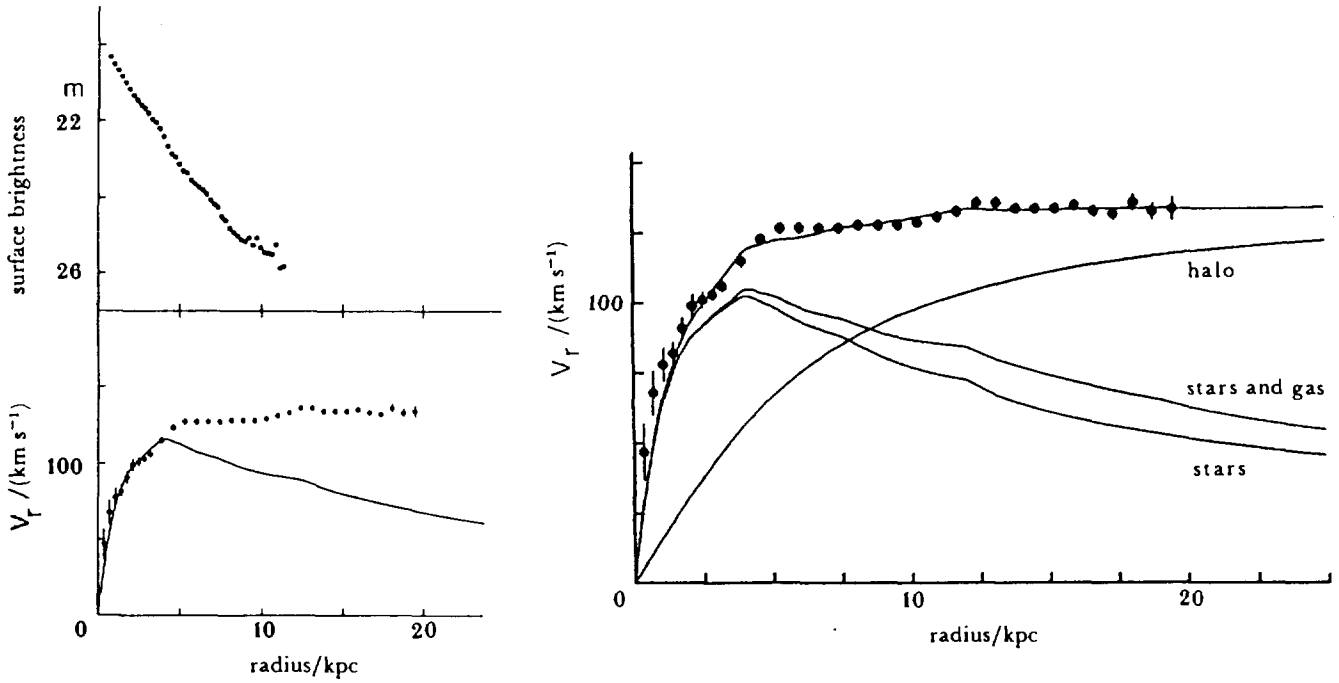

(a) (b)

Fig. 1. Surface brightness (in magnitude) and rotation curve for the NGC 2403 galaxy (a) and its analysis into components. The solid line in fig. a is calculated with l=1.9 and includes correction for H I and He. Note that the vertical scale of the brightness is logarithmic. (Ref. 2)

According to the Newtonian law of gravitation for a central mass M(r) inside the radius r the rotation speed is

$$v(r) = \left[\frac{G\,M(r)}{r}\right]^{1/2} \qquad (1.1)$$

where G is the gravitation constant. For radii for which v is nearly independent from r, M(r) must be proportional to r, i. e. the mean spherical density decreases as $1/r^2$. In fact, as the upper part of fig. 1a shows, the brightness of the disk, thus the luminous matter decreases faster (exponentially) versus radius. In order to fit the measured rotation curve, a non-visible dark matter has to be disposed, the relative importance of which, with respect to the luminous matter, increases with the radius.

Several questions arise at this stage.

1) The radial distribution of the dark matter being defined by the rotation curve, what can we tell on its distribution perpendicular to the disk?
2) Does this dark matter rotate around the galactic axis?
3) What is the nature of this dark matter?

1.1 Axial distribution of the dark matter of the Galaxy

The first determination of the axial distribution of the dark matter is due to Bahcall [3]. From the speed distribution of some tracer stars outside the galactic plane, he concluded that the ratio of the dark to luminous matter densities ρ (dark)/ρ(luminous) lies between 0.5 and 1.5, and this dark matter could be distributed in the same manner as the luminous matter in the disk. More detailed analyses of tracer items, including globular cluster velocities, and especially the neutral hydrogen flaring -in the Milky Way, as in other galaxies- show, that the velocity dispersion does not increase perpendicularly to the disk with the radius, so the total mass distribution is more or less spherical. This does not

exclude a certain flattening of the dark matter halo: though a spheroidal distribution or a thick disk, of at least a few kpc is possible, a spherical symmetry remains the most simple hypothesis. Arguments for the stability of the disk favour also a rather spherical halo.

1.2 Rotation of the halo.

The bulge contains older stars than the disk. It is reasonable to accept that objects farther from the galactic centre have been accumulated later by the Galaxy. The halo could have been accumulated by the same time, or even later than the disk. The luminous galactic halo rotates at about 50 km/s (in the Sun's neighbourhood). If the dark halo is spherical, it is possible that it does not rotate; if it rotates, its axial distribution must flatten. We can accept that the dark halo does not rotate faster than the luminous one, so $v_{r,halo} < 50$ km/s.

1.3 Nature of the galactic dark matter.

The nature of the dark matter in the Galaxy is not independent of the dark matter of the Universe. Without entering into a detailed discussion of the matter density of the Universe, we can retain two figures.

The critical density of the Universe with a Hubble constant of $H = 100\ h$ km/s/Mpc (with $h = 0.75$) is about 6300 eV/cm^3 . This density is several orders of magnitude lower than the luminous density of the galactic disk around the Sun, due to the high concentration of the matter in a galaxy, and especially in the arms of the thin disk of a spiral galaxy. Eq. 1.1 allows to fit from $r_\odot = 8.5$ kpc and $v_\odot = 220$ km/s the mean spherical density of matter around the Sun as $\rho_\odot = 8.5 \times 10^{-25}$ g/cm^3 = 0.46 GeV/cm^3. Comparison of this figure with the luminosity curves suggests that about 0.3 GeV/cm^3 of this matter is dark. Even if this halo is distributed in spherical symmetry in the Milky Way, its density is more than 10000 times higher than the mean critical density of the Universe.

Three main types of matter are considered in most hypotheses.

i) Baryonic matter composed from neutral gas or massive compact halo objects (MACHOs).
ii) Hot dark matter, as e.g. massive neutrinos.
iii) Cold dark matter: Exotic particles, as axions or weakly interacting massive particles (WIMPs).

i) Baryonic halo, with a nearly spherical distribution is known as luminous matter in the Galaxy. Dark matter could contain cold molecular hydrogen (H II) or massive compact objects. (H I is detected through its 21 cm wavelength radio emission.) In order to remain optically undetected, the molecular hydrogen gas must be in thermal equilibrium with the 2.7 K cosmic background. It is, however, difficult to imagine, why this halo, which should exist even in the proximity of hot stars, wouldn't exhibit absorption or emission spectra. It is also doubtful, that this hydrogen gas, which should have in this context more mass than the luminous mass of the Galaxy, does not condense to form stars. For these reasons, the baryonic dark matter is searched rather as massive objects: black holes, brown dwarfs, or faint stars. Very great mass black holes can be ruled out by the regularity of the rotation curves, which would be perturbed by the presence of too big masses.

Two lectures of this school deal with gravitational lensing. So, we just outline the results of microlensing experiments. The evaluations of EROS and MACHO collaborations show that the compact baryonic dark matter in the Galaxy is scarce in the mass region between 10^{-6} and 10^{-1} times $M_\odot$; on the contrary, objects of about 0.5 $M_\odot$ may give a total contribution of as much as 2×10^{11} $M_\odot$ to the halo inside a radius of 50 kpc [4-7]. (Remember, that the total Galaxy mass is estimated $\sim 7 \times 10^{11}$ $M_\odot$.) Unfortunately, as the total number of events (after rejection of spourious cases) is only 2 for EROS and 6 for MACHO, these experiments cannot establish the proportion of Machos in the dark matter.

Conceptual and experimental objections arise against a pure baryonic dark matter. If this matter, representing about 5 times the luminous one is identical to that contained in the disk, it is difficult to explain, why this matter does not exhibit the same spatial distribution as luminous matter, which would be incompatible with the rotation curves. On the other

hand, the primordial nucleosynthesis limits also the baryonic dark matter in the Universe (see P. Salati's lecture). Deuterium proportion in the cosmic hydrogen gas is a sensitive measure of the total baryonic content of the early Universe, and the D/H ratio can be measured through the hyperfine quasar absorption spectrum as far as redshifts of z = 3.2 [8]. Though the evaluations contain some uncertain input data, recent surveys [9-10] of D/H and Li/H ratios claim that the ratio Ω_B of the baryonic to the critical mass density of the Universe (with h = 0.75) should not exceed 6-7 %.

Let us look somewhat out of our Galaxy at least at the local cluster of galaxies. Narlikar presents a careful analysis of mass to light ratios l up to the Virgo supercluster. Again with the same Hubble constant, as previously, it comes out, that the larger structures exhibit higher mass deficit than the smaller ones (cf. Table 1, from ref. a)

Object	l
Milky Way (inner part)	8(3)
Spiral galaxies	12(1)
Local group	220(110)
Local superclusters	110(40)
Abell clusters	650(250)

Table 1. Mass to light ratios for some extended objects.

The luminosity of a great number of galaxies is well known. Knowing also the density of the galaxies, a mean galactic luminosity density can be derived from astronomical measurements: $L_G \sim 1.7 \times 10^{8}$ $L_\odot/Mpc^3$ = 2.2×10^{-39} W/cm^3 .

The critical density of the Universe (1.2) $\rho_c = \frac{3H^2}{8\pi G} = 2.10^{-29}$ h^2 g/cm^3 = 1.1×10^{-29} g/cm^3 = 6.3 GeV/m^3 can be combined with the previous luminosity figure, giving for the mean density of galactic matter in the Universe $\rho_G = 1.1 \times 10^{-32}$ l g/cm^3 $= 6.3 \times 10^{-3}$ l GeV/m^3 and combining this value with the critical density:

$$\Omega_G = (\rho_G / \rho_c) \sim 10^{-3} \text{ l} \qquad (1.3)$$

This expression means, that in order to satisfy the conditions of a flat Universe Ω =1, 99.9 % of the matter is non luminous. As the Galaxy stability requires only l=5-10, the nucleosynthesis limit of Ω_B <7% does not forbid that all matter inside a galaxy should be baryonic, as it is possible from microlensing experiments. It is, however, very unlikely that,while the Universe contains different kinds of dark matter, only the baryonic should be present in the galaxies.

As we shall deal hereafter with a laboratory experiment, we admit that, if non-baryonic matter is present in the Universe, it should be also in our Galaxy, near the Sun.

ii) Dark matter is called hot when the dark matter particles move with relativistic speeds. Light neutrinos were favoured, because they do not introduce new, unknown particles. If electron neutrinos had a rest mass $m_{\nu_e} > 30$ eV, they could fill in the cosmological mass deficit; it would be, however, difficult to understand how these fast particles could condense gravitationally in the galaxies to satisfy the rotation curves. Anyhow, recent electron neutrino mass determinations set a limit of $m_{\nu_e} < 1$ eV, and a new experiment (NEMO III) under installation in the underground laboratory of Modane (LSM) aims to lower this limit to 0.1-0.2 eV. Majorana neutrinos with masses up to some hundreds of GeV and heavy Dirac neutrinos up to TeV are also considered, but the structure function of the Universe could not be reproduced with exclusively hot dark matter [11].

iii) Cold dark matter is composed from particles moving slowly with respect to the velocity of the light.

a) Axions were proposed to solve the strong CP problem, introducing a PQ symmetry which can be broken spontaneously. The axion is associated to this broken symmetry. An axion can interact with two photons and this coupling is strengthened in a strong magnetic field. Cosmological constraints give $m_a > 3 \times 10^{-5}$ eV, while the neutrino signal from the supernova SN 187a limits axion mass to smaller than a few times 10^{-4} eV. For 10^{-4} eV the photon frequency is of the order of 10 GHz, and so this interaction could

be detected in a tuned microwave cavity. Experiments in progress didn't show any resonant signal till now.

b) Supersymmetric dark matter.

The supersymmetric theories (SUSY) allow the existence of a great family of new particles. These particles are not in contradiction with the standard model, and are expected to have masses higher than the nucleonic mass. SUSY works with a basic symmetry between fermions and bosons, and assigns a superpartner to each known particle: a superboson to a fermion and a superfermion to a boson. The vocabulary of superparticles is the following:

-if the ordinary particle is a boson, (e.g. a photon γ), its supersymmetric partner takes the name of this boson with a suffix ino: photino ($\tilde{\gamma}$).

-if the ordinary particle is a fermion, (e.g. a neutrino ν) its supersymmetric partner takes a prefix s: sneutrino ($\tilde{\nu}$).

As ordinary particles, the heavier supersymmetric particles decay to the lighter ones. In order to form the dark matter, these particles had to survive since the big bang. The most probable hypothesis is that the lightest supersymmetric particle (LSP) should be stable and neutral (as it has not been detected through an electromagnetic interaction). SUSY calculations confronted to high energy physics experiments suggest that this particle is the neutralino (χ), a particle of spin 1/2, being its own antiparticle (Majorana fermion). The neutralino can be obtained from a linear combination of 4 neutral spin 1/2 supersymmetrical particles: photino ($\tilde{\gamma}$), zino ($\tilde{z}$), and two higgsinos ($\tilde{h}_1$ and $\tilde{h}_2$).

2. Supersymmetric dark matter.

2.1. WIMP mass, density and interactions.

Supersymmetry breaks at an energy of the order of a TeV, thus the LSP should have a mass lower than this value. Cosmological considerations combined with SUSY annihilation cross sections establish at the same order the upper limit of the LSP mass. A recent contribution of the ALEPH collaboration at LEP establishes a lower limit of the neutralino mass: In the minimum supersymmetric model and with a reasonable ensemble of parameters (e.g. $m_{\tilde{\nu}} > 220$ GeV/c^2), in the 95 % confidence limit $m_\chi > 12.8$ GeV/c^2 , and with some larger hypotheses $m_\chi > 34$ GeV/c^2 [12].

Up till now no experiment could prove the existence of such a supersymmetric particle. It is clear from the observational difficulty, that the LSP does not interact with the ordinary matter neither through nuclear forces, nor by electromagnetic interaction. Only two interactions with ordinary matter can exist: the gravitational and the weak interactions. Therefore, these particles are called Weakly Interacting Massive Particles (WIMPs). In fact, axions, heavy neutrinos and some other exotic particles are also WIMPs, but this denomination is usually reserved in astrophysics to the supersymmetric massive particles.

Let us roughly estimate the cosmological abundance of the WIMPs which, by the time of the big bang, were not all LSP. Thermal equilibrium with the Universe being at a temperature of T means that $m_\chi c^2 < kT_u$ and the annihilation to a lighter particle pair $\lambda\bar{\lambda}$ ($X\bar{X} \rightarrow \lambda\bar{\lambda}$) is compensated by the inverse $\lambda\bar{\lambda} \rightarrow X\bar{X}$ reaction. When the expansion rate of the Universe H becomes higher than the reaction rate, the equilibrium breaks and a relic abundance of X is maintained.

The reaction rate depends on the mean cross section of annihilation $\langle\sigma_A\rangle$. Without entering into detailed calculations of this relic abundance, it is qualitatively clear that the present cosmological density Ω_χ of LSP -which remains after the decay of heavier X- will be higher for lower expansion rate H and for lower annihilation cross section. With h~0.75 and estimating $\langle\sigma_A\rangle$ we find that for an age of 13 Gyears of the Universe $\Omega_\chi h^2 < 0.4$, and if the Universe is flat ($\Omega = 1$), the constraint becomes even stronger $\Omega_\chi h^2 < 0.25$. With the previously adopted value of h the relic density of the WIMPs becomes $\Omega_\chi < 0.5$. The new cosmological cookery recommends therefore, in agreement with the proven existence of baryonic dark matter and with its primordial nucleosynthesis limit, and with a possible hot dark matter contribution, to take as ingredients to the Universe 10 % of baryonic, 20 % of non baryonic hot and 70 % of non baryonic cold dark matter.

As for the galactic dark matter, with the above considerations, and ta-

king a nearly spherically symmetric halo, $\rho_\chi = 0.3$ GeV/cm^3 is adopted in the vicinity of the Sun.

2.1 Possibility of the detection of the WIMPs.

The direct detection of the WIMPs makes use of the elastic scattering cross section of WIMPs on the target nuclei of a particle detector. The detected energy spectrum depends on:

1) the differential cross section of energy tranfer WIMP-nucleus $d\sigma/dW$
2) the relative velocity v of the WIMP with respect to the target.

2.2.1. Cross section considerations.

The elastic scattering of a WIMP on a nucleus is based on the interaction of a WIMP with the quarks and the gluons. The amplitude of the WIMP-gluon interaction is related to that of the annihilation cross section of WIMPs to quarks. This is the most uncertain term in the cross section estimation.

The quarks and gluons tranfer the interaction to the nucleon. This part of the interaction is somewhat better known from high energy accelerator experiments.

The nuclear wave function takes into consideration the interactions between nucleons and their distribution in the nucleus. This term is represented by a global nuclear form factor F depending on the proton and neutron form factors, which are rather well known from electron scattering experiments on nuclei.

The probability of transferring W energy, $d\sigma/dW$ can be represented in a simplified way as

$$d\sigma/dW \sim \sigma_o f(W) \qquad (2.1)$$

where σ_o describes the basic interaction processes and f(W) depends only on kinematic quantities, as masses, relative speed and scattering angle Θ in the centre of mass frame

$$\frac{\Delta W}{W} = \frac{2m_r}{m_\chi m_N}(1-\cos\Theta) \qquad (2.2)$$

where m_χ and m_N are neutralino and scattering nucleus masses and

$$m_r = m_\chi m_N/(m_\chi + m_N)$$

is the reduced mass. As the transferred energy is small, the diffusion is isotropic.

The total cross section can be expressed as $\sigma_o = 4G_F^2 m_r^2 C \qquad (2.3)$

where G is the weak interaction constant and C describes the interaction between the neutralino and the nucleus.

The WIMP-nucleon interaction may be scalar, vectorial or axial (spin dependent). When the WIMP is a Majorana fermion, as the neutralino, no vector interaction is present [13]. For axial (spin dependent) interaction

$$C_{SPIN} = \frac{8}{\pi}\Lambda^2 I(I+1) \qquad (2.4)$$

where I is the nuclear spin and Λ contains all the terms describing the basic interactions. (For the units see footnote at the end of this paper.)

For a scalar interaction

$$\sigma_{o,SC} = \frac{4}{\pi}\frac{m_r^2 m_N^2}{m_N^2} l^2 \qquad (2.5)$$

where m_n is the nucleonic mass and l contains the WIMP-nucleon coupling.

The evaluation of Λ and l is very complicated as, even for the acceptable cosmological and elementary particle physics constraints concerning the neutralino, several thousands of models can be considered. It is, however, possible to derive some general considerations from eqs. (2.4) and (2.5).

i) Scalar interaction is coherent, so its cross section increases strongly with the nucleonic number of the target nucleus. This is not the case for axial coupling. For light nuclei the axial coupling can dominate, while for A>50 the scalar one becomes more important. Nevertheless, the cross section depends strongly on the ensemble of the chosen parameters. For ^{73}Ge, for instance, the scalar to spin interaction ratio R seems to be around 30, but different models allow 1<R<300.

ii) Cross sections are of the order of 10^{-38} cm^2, or even smaller. This yields an extremely low detection rate, typically 0.01-0.1 event/kev/kg/day

of detector mass. Usual background radiation gives several orders of magnitude higher detection rates. We shall come back later to this point.

2.2.2. Velocity considerations and rate of events.

The rate of events R per unit mass of detector, interacting with neutralinos is proportional to $R \sim nv\sigma(v)$, where n is the number of neutralinos in a unit volume. $n = \rho_\chi / m_\chi$, and for the dark matter $\rho_\chi = 0.3$ GeV/cm^3. The rate of transfer dR of an energy W to the nucleus for unit mass of detector will be

$$dR = A \frac{\rho_\chi}{m_\chi m_N} v f(v) \frac{d\sigma}{dW} dW\, dv \qquad (2.6)$$

where dW can be taken from (2.2), v is the relative velocity between the target nucleus and the WIMP, and f(v) is the normalized distribution of these velocities; the constant A contains Avogadro number, the specific weight of the detector, and the isotopic abundance of the considered target element.

The velocity $\vec{v}$ is $\vec{v} = \vec{v}_h - (\vec{v}_\odot + \vec{v}_E)$ where v_h is the velocity of the halo dark matter particles, $\vec{v}_\odot$ the solar rotation speed in the Galaxy and $\vec{v}_E$ the rotation speed of the Earth around the Sun.

Before the condensation of the Galaxy the baryonic and the cold dark matter were in thermal equilibrium. According to the virial theorem, this equilibrium implies a speed distribution of $f_h \propto \exp(-v_h^2 / v_\infty^2)$ [14], conserved during the condensation into a galaxy, where v_∞ is the Galaxy's rotation speed at $r \to \infty$, which does not differ much from $v_\odot$. In the isotropic halo model the dispersion of the velocity v_h is equal in the disk plane and perpendicular to it. The distribution function f_h must be cut at velocities $v_h > v_{esc}$, the escape velocity from the Galaxy, which can be estimated from astronomical observations to 650-850 km/s.

Velocities of the Sun in the Galaxy and of the Earth in the solar system have to be substracted vectorially. Considering the tilt angle of the ecliptic plane with respect to the galactic disk, and a particular movement of the Sun in the disk, one finds a yearly modulation of $|\vec{v}_\odot + \vec{v}_E|$ between a minimal speed the 4. dec (~226 km/s) and the maximal one the 2. June (~255 km/s). This speed modulation changes slightly the event rate, and especially its energy spectrum: A summer-winter asymmetry of a few percents can be attained. This modulation, if observed, could be considered as a clear signature of the neutralino-nucleus interaction.

For a given neutralino mass and relative speed v the deposited energy is distributed around v^2; though we have a reasonable hypothesis on the velocity distribution, we don't know the neutralino mass m_χ. As the rotation curve defines the mass density $\rho_\odot$, the number of neutralinos n with mass m_χ is inversely proportional to m. The observed spectrum versus deposited energy R(W) can be transformed to the rate versus mass relation $R(m_\chi)$, which decreases strongly with m_χ.

Unfortunately, the background radiation spectrum shows a similar shape (cf. fig 6). So it is crucial to diminish the background counting rate below that estimated for neutralino-nucleus interactions, and observe then the modulation described previously.

3. Bolometric detection.

In principle, any nuclear counter can be used for dark matter detection. The requirements are, however, severe.

i) Low radioactive pollution of the detector and its surrounding.

ii) Low sensitivity to background radiation (essentially gamma radiation), or the possibility to reject such events.

iii) Very low noise level, i.e. good energy resolution.

iv) Possibility to produce large mass detectors.

The energy deposited in a detector may be transformed into 3 kinds of signal:

1) Electrical signal, as in gaseous or semiconductor counters. In general, less than 30 % of the particle energy is converted into charges.

2) Light signal (scintillation) in scintillation counters. Only less than 10 % of the particle energy is converted into light. The conversion of the light to an electric signal has also a ~10 % efficiency.

3) In any case, the greatest part of the absorbed energy is degraded into heat. A small fraction of energy may be stored as excitons in excited

solid state levels.

When the number of information carriers N_c is small, the relative energy resolution $\delta W/W$ is proportional to $1/N_c$, hence the interest of increasing N_c. The carriers of the heat signal are the phonons. When they are in a thermal equilibrium with the crystal, their energy W_{ph} must be lower than the Debye energy of the crystal kT_D, where T_D is the corresponding Debye temperature. Typical orders are $T_D \sim 200$ K, $W_{ph} \sim 30$ meV yielding thus $N_c \sim 3\times10^4$/keV. The direct detection of the heat is realized in bolometers. As bolometers operate at low temperature, the actual phonon energy is even lower. E.g. for a sapphire crystal operated at 55 mK, the mean phonon energy is only 1.3×10^{-5} eV.

When a neutralino strikes a nucleus of the target, it ejects the nucleus of its site. The moving nucleus becomes a heavy ion and it will be slowed down. The slowing down, characterized by the linear energy transfer (LET) is greater for heavy particles than for electrons (produced from radiation-material interaction) after the absorption of a gamma ray. The charge collection in semiconductors, and even more the light efficiency in scintillators, decrease with increasing LET. The ratio of the charge (or electric) signal from a heavy particle with respect to the charge (or electric) signal of a gamma ray is called the quenching factor Q. Fig. 2 shows the quenching factor for a CsI(Tl) crystal versus the energy of the recoiled nucleus.

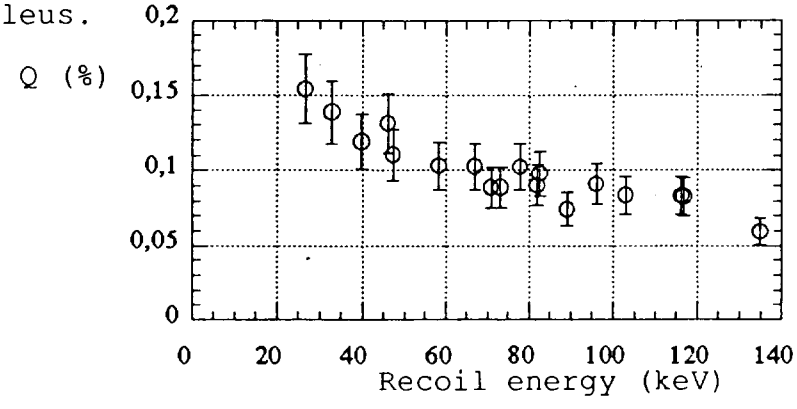

Fig. 2. Quenching factor at room temperature of a CsI(Tl) crystal [16] The Cs and I ions were recoiled by fast neutrons.

The greatest part of the absorbed energy ΔW heats the crystal:

$$\Delta T = \Delta W / C \qquad (3.1)$$

where C is the heat capacity of the crystal having mass M:

$$C = M\,[\alpha T + \beta (T/T_D)^3] \qquad (3.2)$$

The first term of (3.2) describes the electronic heat capacity. This term is overhelming in metals, but in hyperpure metal-free crystals it is negligible. The second term describes the phononic heat capacity. In order to obtain a high heating up ΔT, C, and thus T/T_D must be $<<1$: a high Debye temperature crystal has to be operated at low temperatures, typically at 10-100 mK. The necessary low temperatures are produced with a ^{3}He-^{4}He dilution refrigerator.

The heating up of the crystal is detected on a sensor, which can be a neutron transmutation doped (NTD) germanium resistor, glued onto the crystal. These resistances increase very strongly with 1/T; typical values are around a few hundreds of kΩ to a few MΩ at the working temperature.

A small electric current polarizes the sensor. When a particle heats the crystal, the elevation of the sensor temperature diminishes its resistance, and the tension changes on the extremities of the sensor. The sensor is coupled through an appropriate heat link -e.g. sapphire block -to the refrigerator. The rise and fall time constants depend on the crystal size and the heat coupling. The first one is, in general, lower than 1 ms, while the fall time is longer than the rise time. Bolometers are slow with respect to semiconductor or scintillation counters, but the counting rate is very low in these experiments.

The internal energy of the crystal is $U = CT$, and its mean fluctuation $\delta U = \sqrt{kT^2C}$, which, with (3.1) and (3.2) gives

$$\delta U = \sqrt{k\beta}\, M^{1/2}\, T^{5/2} \qquad (3.3)$$

and the fundamental limit of the resolution is $\delta W \sim \delta U$

The obtained signal is linear with the absorbed energy, as long as $W << U$ (the absorbed energy is small with respect to the internal energy of the crystal).

In practice, the resolution is, unfortunately, much worse than that given by the fundamental limit. Hereafter we give some of the reasons.

i) Amplifier noise which is proportional to the squareroot of the transmitted frequency band Δf.

ii) Electromagnetic induction due to the network, radio and television emitters, ground loops, etc.

iii) Mechanical vibrations. Theses vibrations can induce directly signals in the wires or, if they are damped, their energy is transformed into heat signals.

iv) Temperature instability. On account of the sharp temperature dependence of the sensor resistance R(T), a fraction p of temperature variation changes the signal amplitude by a fraction of 2p about. For example, if T=20mK and the temperature shift is 50 μK, a typical -line of W=5 MeV will be broadened to δW=25 keV. This line broadening which is proportional to the energy is particularly important for long running times. For a continuous spectrum, as that of WIMPs, the temperature instability flattens the spectrum slope (cf. annual modulation of the neutralino-recoil spectrum!).

4. Background reduction.

The greatest part of the background radiation comes from the nature: radioactivity of the environment, of the cryostat and detector materials, and cosmic rays. The first protection is a passive one: to absorb sufficiently the penetrating radiation (e.g. cosmic muons), the experiments are realized in underground laboratories. In Tables 2. and 3. we give some comparative background data in the motorroad tunnel of Frejus (LSM) situated at 1200 m above the sea level under the Mt. Frejus at the French-Italian border [17,18].

	Sea level	LSM
Water equivalentdepth (m)	0	4400
Fast neutron flux (W_n > 1 MeV) (/cm^2 s)	}	4×10^{-6}
Thermal neutron flux	0.2	1.6×10^{-6}
Muon flux	150 /m^2 s	4 / m^{2}day

Table 2. Particle flux attenuation in LSM

The continuous gamma background, measured with a 100 cm^3 Ge detector is reduced by about a factor of r at energy W with respect to the sea level:

W(MeV)	r
0.2	1.5
0.4	2
1.0	3
Radon content of air	~ 10-15 Bq/m^3 (under ventilation)

Table 3. Continuous gamma background attenuation in LSM.

The reduction of the muon flux is an important factor for large bolometers. Most of the sea level muons have energies near the minimum ionization energy ~300 MeV, and as their energy loss is of the order of 1 MeV/(g/cm^2), the energy deposited in the detector, 20-50 MeV, gives such a great heating, that the recovery time of the detector, i. e. its baseline restoration may take more than a second.

The continuous gamma background is due to the Compton scattered gamma rays of the natural radioactivity, mainly of elements of the Th and U series and from ^{40}K. A good underground laboratory must be rather in a limestone, than in a granitic mountain. The detector has to be protected against gamma background with copper and/or archeological lead. Such an assembly is shown on fig. 3.

An active protection against gamma ray background can be achieved making use of the quenching factor of the recoil nuclei. For the par-

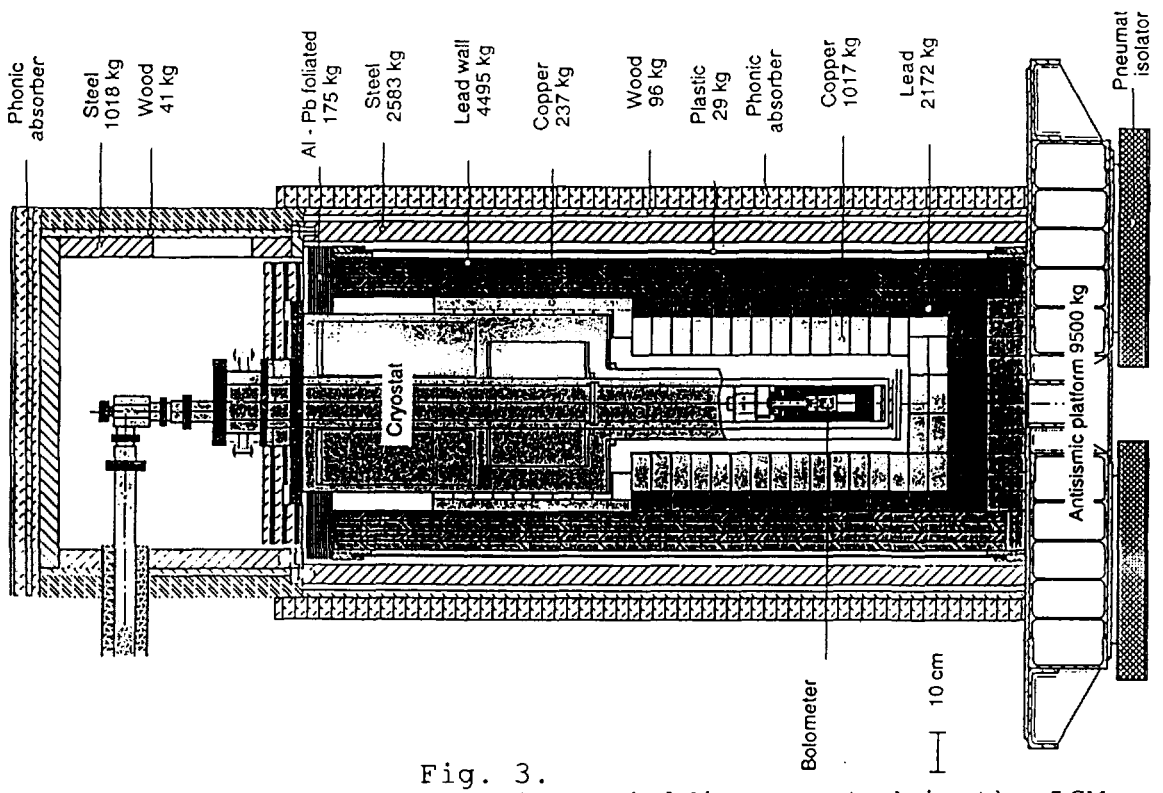

Fig. 3.
Cryostat assembly with radiation shielding mounted in the LSM. Archeological lead is disposed around the bolometer.

ticle-gamma ray discrimination two quantities have to be measured simultaneously: the heat signal of a bolometer crystal, and a second one: either the collected charge in a semiconductor, if the bolometer crystal is a Ge, or the emitted light, if the bolometer is a scintillating crystal. The two strategies correspond to the two possible interactions: the coherent (scalar) interaction is efficient in heavier nuclei (Ge), while the axial interaction is strong for instance on fluorine (CaF_2 scintillating crystal). Both possibilities are under development. In fig. 4 we show the scheme

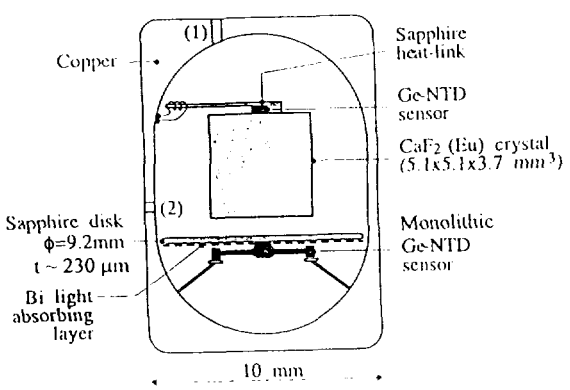

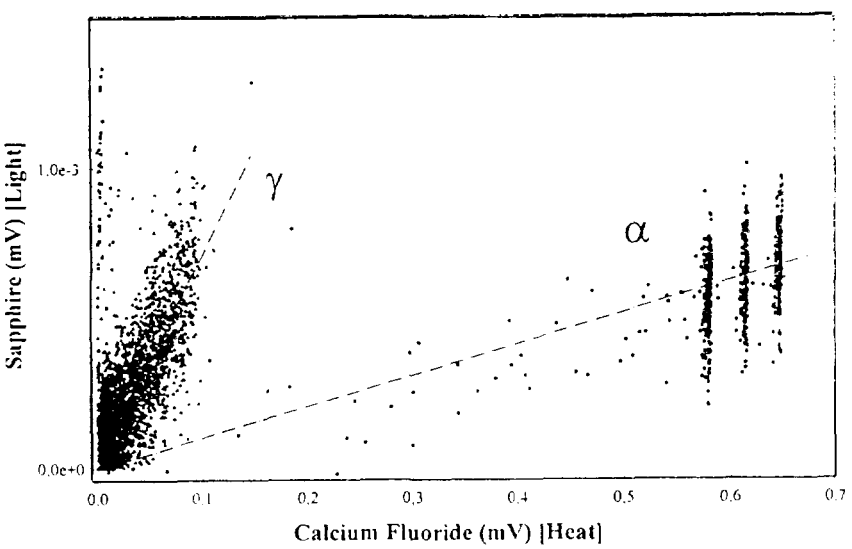

Fig. 4.
Double scintillating bolometer. The great crystal is a CaF_2 (Eu) scintillator. The fluorescent light of the CaF_2 is absorbed in the Bi layer of a thin sapphire infrared bolometer.

Fig. 5.
Identification plot of the double scintillating bolometer.
Horizontal axis: CaF_2 pulse height (heat)
Vertical axis: sapphire " " (light)
- source: $^{239}Pu + ^{241}Am + ^{244}Cm$
- source: ^{60}Co

Events out of the main lines are due to scattering on the surrounding material.

thin sapphire infrared bolometer [19]. Fig 5 shows the first results of such a double bolometer, tested with 3 alpha lines and a ^{60}Co source; the vertical dispersion of the points is due to vibrations of the refrigerator system (cf. horizontal and vertical scales!). The total rejection rate of gamma pulses above 150 keV is about 70 %.

Other rejection procedures can be employed in NaI(Tl) scintillation counters. The scintillation is produced in different (at least two) F-centres, with different decay times. The relative intensities of the excitation of each of theses centres depend on the ionization density, thus on the nature of the ionizing particle. So, the analysis of the pulse shape allows the rejection of the gamma background

5. Exclusion plots and perspectives.

We represente on fig. 6 the background spectrum measured in the assembly of fig. 3, with a 24 g sapphire bolometer. This bolometer has no active background rejection, and on account of its small dimensions, its low energy γ-background related to its mass, is high. This plot can be transformed, as described in par. 2, to cross section versus neutralino mass exclusion curves. The measured interaction cross section is the sum of scalar and axial interaction cross sections. The ratio of scalar to axial cross sections σ_o(scalar)/σ_o(axial) scales as A^2. In order to compare measurements performed with different detectors, the cross section represented on the vertical axis is the neutralino-nucleon (and not the neutralino-nucleus) one, supposing that the considered interaction is dominant. Using $v_\odot$ =220 km/s, $\sqrt{<v^2_{halo}>}$=270 km/s, v_{esc} =800 km/s and ρ_x = 0.3 GeV/cm^3, curves labelled 1 in figs. 7 a and b show the σ(W) relations if events of fig. 6 were due to neutralino-nucleon interactions. Some other measurements are also represented for comparison. In fact, the measured background countings are about 100 times above reasonable theoretical cross section estimates. The presented curves are to be considered as exclusion contours, allowing any relation situated below the curves.

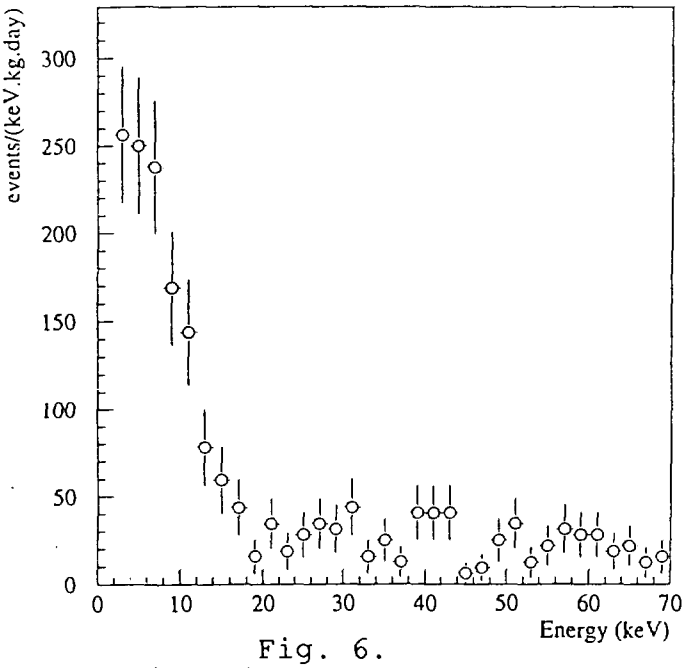

Fig. 6.
Radioactive background spectrum.

The everage rate above 16 keV is 25 evts/kg/keV/day.

Large volume detectors with active gamma-background rejection are in developpement in several laboratories. We represente on fig. 7a an exclusion curve simulating a 100 days experiment with a 75 g discriminating Ge bolometer. This detector is now operational, it is being tested in LSM. Another Ge detector is under installation in a mine in Soudan (USA). Greater volume Ge detectors are currently used in nuclear research: their use as bolometers can be achieved in the near future. We continue also the development of a greater scintillating bolometer, in order to favour the axial neutralino-nucleon interaction.

Should we believe that the major part of the Universe is composed of a matter different of that we are from, and escaped our observation till now, or is the solution of the cosmological mass deficit elsewhere? The challenge is exciting, and the only answer an experimenter can give is: work and see.

Footnote. Cross sections are given in $\hbar$=c=1 units, often employed in particle physics. The correspondance with usual units is 1 fm = 5.07/GeV.

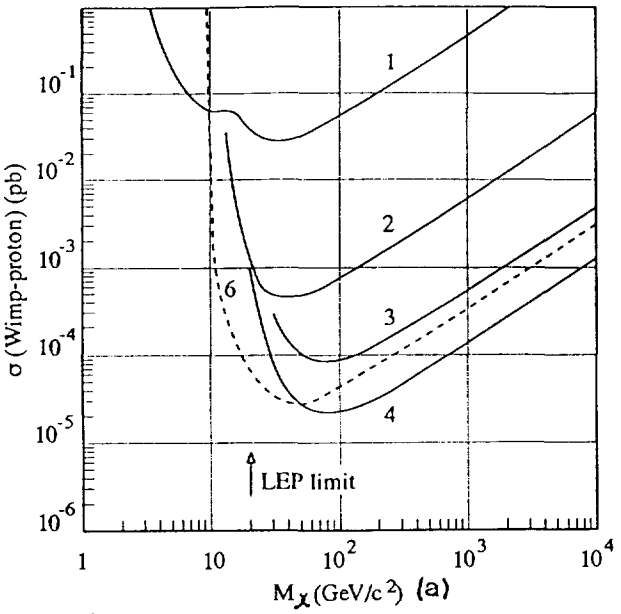

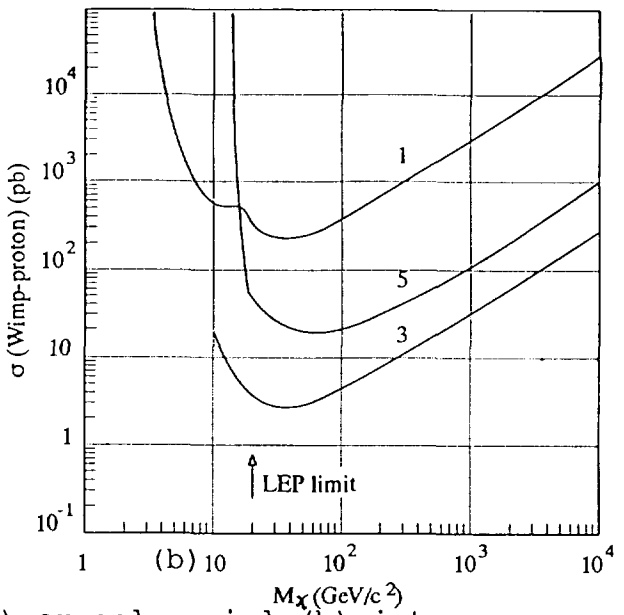

Fig. 7. Exclusion plots for only scalar (a) or only axial (b) interaction from some measurements [Ref. 15 and G. Nollez private communication.]

1.	24 g	Al_2O_3	Bolometer	EDELWEISS col	LSM lab	1995
2.	340 g	TeO_2	Bolometer	Milano	Gran Sasso lab	1996
3.	6 kg	NaI	Scintillator	Oxford-Rutherford	Boulby mine lab	1995
4.	2.75 kg	Ge	Semiconductor	Heidelberg-Moscow	Gran Sasso lab	1994
5.	380 g	CaF_2	Scintillator	BPRS coll.	Mentogou lab	1995
6.	75 g	Ge	Bolo-semic.	EDELWEISS col	LSM lab	simulation

References (general)

a. J.V. Narlikar: Introduction to cosmology (Cambridge Univ. Press)
b. P.J.E. Peebles: Principles of physical cosmology (Princeton series in physics, PUP, 1993)
c. L. Gouguenheim: Méthodes de l'astrophysique (Hachette, Paris 1981)
d. L.M. Celnikier: A la recherche de la quintescence, Bull. Soc. Fran. Phys. No 96 (1994) 12
e. P.F. Schmidt & J.D.Lewin: Dark matter detection Phys. Rept. 187 (1990) 203
f. V. Tremble: Existence and nature of dark matter in the Universe, An. Rev.Astroph. 25 (1987) 425
g. J.R. Primack, D. Seckel & B. Sadoulet: Detection of cosmic dark matter, An.Rev.Nuc.Part.Sci. 38 (1988) 751
h. G. Jungman, N. Kamionkowski & K. Griest: Supersymmetric dark matter, Phys. Rept. 267 (1996) 195
i. L. Mosca: Dark matter direct detection, XXXI Rencontres de Moriond, to be published.

References (particular)

1. E.I. Gates, G. Gyuk & M.S. Turner, Phys. Rev. Let. 74(1995)3724
2. T.S. Van Albada & R. Sancisi, Phil. Trans. Roy. Soc. Lond. A320(1986)447
3. J.N. Bahcall, Phil. Trans. Roy. Soc. Lond. A320(1986)543
4. B Paczynski, Astroph. J. 304(1986)1
5. E. Gates & M.S. Turner Phys. Rev. Let. 72(1994)2520
6. C. Alcock et al (MACHO col) Phys. Rev. Let. 74(1995)2867, Astroph. J. 445(1995)133, ibid 449(1995)28. ibid. 461(1996)84
7. R. Ansari et al (EROS col) Astron. & Astroph. 314(1996)94
8. A. Songaila, L.L. Cowie, C.J. Hogan & M. Rugers, Nature 368(1994)599
9. C.J.Copi, D.N. Schramm & M.S. Turner, Science 267(1995)192
10. P.J. Kernan &. S. Sarkar, Phys. Rev. D54(1996)R3681
11. S.D.M. White, C.S. Frenk & M. Davies, Astroph. J. 274(1983)L1
12. ALEPH col., CERN PPE/96-083 Rept. to be published in Zs. f. Phys. C
13. H.E. Haber & G.L. Kane, Phys. Rept. 117(1985)75
14. A.K. Drukier, K. Freese & D.N. Spergel, Phys. Rev. D33(1986)3495
15. A. de Bellefon et al (EDELWEISS col.) to be published in Astropart. Phys.
16. Rept. ULTIMATECH, Lyon 1996 (unpublished)
17. V. Chazal, Ph. D. thesis, Lyon, 1996.
18. Ph. Hubert, unpublished.
19. Ch. Bobin et al. to be published in Nucl. Inst.&Meth. A.